UCRL-JC-132257
PREPRINT

Performance Results on the Laser Portion of the Keck Laser Guide Star System

H. W. Friedman, J. B. Cooke, P. M. Danforth,
G. V. Erbert, M. Feldman, D. T. Gavel,
S. L. Jenkins, H. E. Jones, V. K. Kanz,
T. Kuklo, M. J. Newman, E. L. Pierce,
R. W. Presta, J. T. Salman,
G. R. Thompson, and N. J. Wong

This paper was prepared for submittal to the
OSA Topical Meeting on Astronomy with Adaptive Optics,
Present Results and Future Programs
Sontehofen, Germany
September 2-4, 1998

September 29, 1998

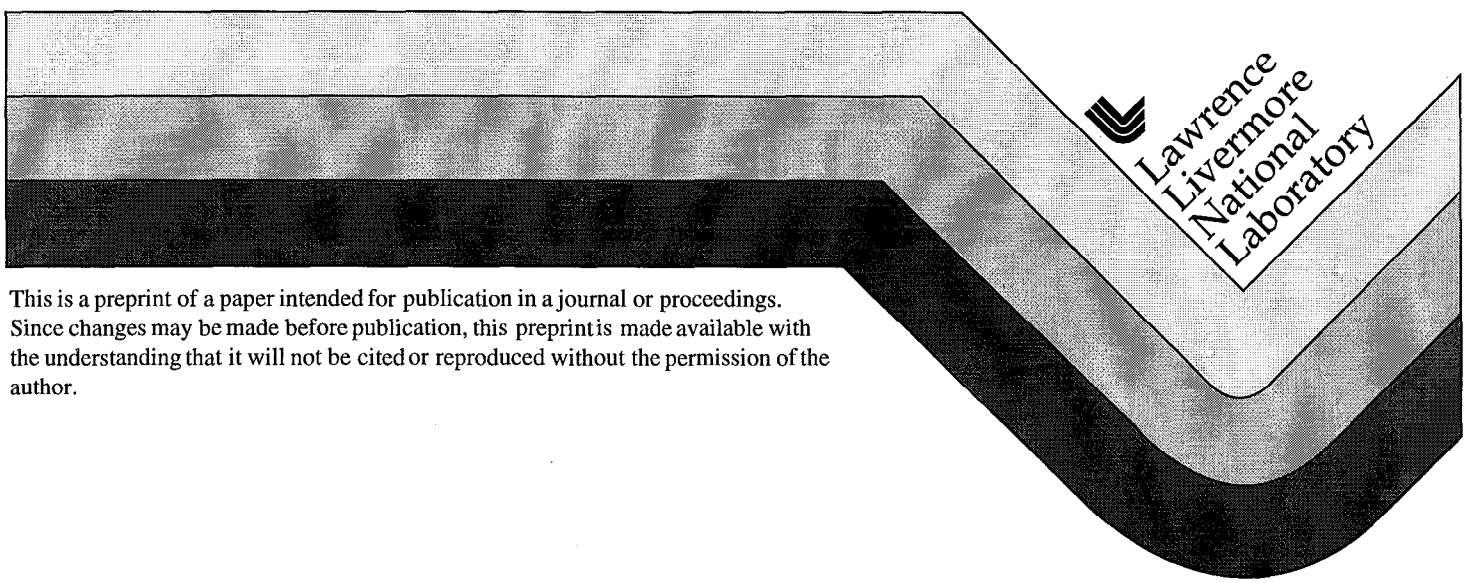

Performance Results on the Laser Portion of the Keck Laser Guide Star System

H. W. Friedman, J. B. Cooke, P.M. Danforth, G. V. Erbert, M. Feldman, D. T. Gavel, S. L. Jenkins, H.E. Jones, V. K. Kanz, T. Kuklo, M. J. Newman, E. L. Pierce, R. W. Presta, J. T. Salmon,G. R. Thompson, N. J. Wong

Lawrence Livermore National Lab
Box 808, L-464
Livermore, CA 94550
e-mail: friedman3@llnl.gov

1. Background

The Laser Guide Star (LGS) system for the Keck II, 10 m telescope consists of two separate but interconnected systems, the laser and the adaptive optics bench. The laser portion of the LGS[1] is a set of five frequency doubled YAG lasers pumping a master oscillator-power amplifier dye chain to produce up to 30 W of 589 μ at 26 kHz of tuned light. Presently the laser system has been set up at the Keck facility in Waimea, HI and is undergoing test and evaluation. When it will be set up on the Keck II telescope, the pump lasers, dye master oscillator and associated control equipment will be located on the dome floor and the dye laser amplifiers, beam control system and diagnostics will be mounted directly on the telescope as shown in Fig. 1. Extensive use of fiber optics for both transmission of the oscillator pulse and the pump laser light has been used.

2. Description of the test.

The goal of this test was to demonstrate "hands-off" operation of the laser system over an 8 hour period, at full power, on wavelength and with good beam quality. The test was performed at LLNL during January 1998. The diagnostics which were operated are the Fabry-Perot Interferometers (FPI) to measure mode quality out of the laser and after the modulator, the vacuum sodium cell to verify that the laser is on wavelength, power meters, the Shack-Hartmann wavefront sensor, Pointing and Centering cameras and the Power-in-the-Bucket (PIB) camera to measure the focal point power distribution, i.e., the "beam quality".

The laser system was started about three hours before the test to let all systems thermally equilibrate and all the diagnostics adjusted. The run lasted about 30 minutes longer than the 8 hours and ended in the evening. The laser system was operated in the normal mode, i.e. with the first YAG laser powering both the GIDMO and the preamp at the full system PRF and the rest of the YAG lasers run in two time sets of half the PRF each. The outputs of these two time sets were interleaved to pump the power amplifier at the full system PRF. The following charts represent the data collected from that run.

3. Average power

The plot shown in Fig. 2 shows the power reading as measured from the fast shutter power meter just after the L3 lens. At the beginning of the test, all 4 YAG lasers pumped the amplifier producing an average power of about 30 W, some of which may have been Amplified Spontaneous Emission (ASE). Rather than try to tune the laser at this power level, it was decided to turn off one of the YAG lasers to reduce the power to about the 20 W level which corresponds to the 10 kW/cm^2 value which was our design point.

It is not clear that the output window would have failed at the 15 kW/cm^2 level corresponding the 30 W but there was no reason to put the window at risk for this test. Recall that the optical fiber length was 110 m corresponding the our initial estimate (plus safety margin) and that the latest measurements indicate a final fiber length of about 70 m, so that with all the lasers running and the fiber trimmed to the minimum length, the power level could be as high as 40 W.

There are two ways to use this margin. The first would be to turn off two YAGs and use them for spares and just operate at the 20 W level. The second way would be to enlarge the beam to a diameter of about 0.7 mm from the present 0.5 mm and regap the amplifier to fit. This would permit operation at somewhat less than the 40 W level since the conversion efficiency

is likely to be less with the larger gap. The latter method is preferred since the higher laser power would give more margin for those times of lower sodium density and poorer atmosphere seeing statistics. The final determination of which method in which to operate the laser should wait until the laser is fitted to the telescope.

According to Fig. 2 , the laser power remained over 16 W for the entire test. There was a small adjustment at about three hours into the test. It was noticed that the power was dropping slightly and an adjustment of the GIDMO beam into the launch fiber recovered the power and this was not adjusted for the rest of the test.

At the end of the test, the fourth YAG laser was shuttered back into the system and the power increased to 23 W. The power did not climb back to the original 30 W because some fraction of that power was probably ASE and adjustments to various apertures rejected that component.

The YAG power output remained constant to about 10% during the run as shown in Fig. 3. The dye conversion efficiency remained between 8-9% as shown in Fig. 4. This efficiency is the dye output power divided by the green power as measured at the YAG lasers and therefore has the fiber loss included. For the 110 m of fiber length, the fiber loss was measured to be about 50% so that the dye conversion efficiency with the fiber loss removed is just below 20% which agrees with previous experience for that stage amplifier.

4. Etalon and wavelength lock loops

The etalon and wavelength lock loops on the waveform generator were cabled according to Fig. 5. The lock loops remained locked for about an hour after the start of the run as indicated in Fig. 6 which chronicles the adjustments made during the run.

There is a proportional valve in series with the primary coolant for the GIDMO heat exchanger and a temperature controller which should regulate the dye temperature in this loop to a few tens of millidegrees C. Unfortunately, this temperature regulator was incorrectly wired (two connection swapped at the multipin connector) and the temperature excursions in the dye were much higher, as indicated in Fig. 6. After some time, the PZT controller for the etalon was out of range and it was necessary to (remote) manually recenter the PZT using the motor stage at which time the lock loop resumed its function.

Two improvements were made prior to shipment of the LGS to Keck, one was to correct the wiring error and the other was to provide the software to off load the PZT control to the motor control when the PZT reached its limit. With the wiring error corrected, the temperature control did indeed maintain the dye temperature to a few tens of millidegrees C so that this off loading problem should be much less severe. In addition, the off loading software (and associated hardware D-A converter) should solve this problem completely.

5. Wavefront sensor

The wavefront sensor based upon a Shack-Hartmann lenslet was operated during the run. A sample of the data produced is shown in Fig. 7. The technique for this measurement uses a reflection from the side of the final lens facing the sky, L4, added to the wavefront of the beam from the laser to determine the entire wavefront error from all the lenses as well as that from the laser. The configuration for this measurement in the laboratory where the final lens was unavailable was to place a lens identical to L3 at a distance from L3 such that the focal point is midway between the two lenses. In this manner, the two lenses form a collimated beam after the second lens. Placing a flat after the second lens and adjusting the tilt to retro the beam back into the system simulates the effect of the L4 lens. Since the L3 is a "best form" plano-convex lens with no true flat, the extra flat was necessary. However, even if a true plano-convex lens were available for L3, the spherical surface would have introduced aberrations and the above described scheme was preferred.

The RMS wavefront error as measured by this sensor is 0.07 waves corresponding to a Strehl of 0.8 which is misleadingly high. This will be shown in the next section where the PIB method is used to measure beam quality. The reason for this unusually high value of Strehl is that the lenslet array does not contain enough elements to measure the high spatial frequency components of the aberrations and therefore overestimates the beam quality.

The diagnostic is still quite useful as an alignment tool because it gives a physical picture of the wavefront. Features such as clipping of the beam on the amplifier cell stand out and are easily identified for corrective action. Also, this diagnostic provides a clear and accurate means of adjusting the L1-L2 and L3-L4 telescopes for focus and astigmatism, i.e. lens tilt.

6. Beam quality diagnostic

A Power-in-the-Bucket (PIB) camera was used to measure beam quality using the diameter of the circle which contains 80% of the total energy as a figure of merit. This test does not include any errors introduced by the L3-L4 combination but does measure the far field of the laser and all the optics up to that lens pair. The Eltec camera has limited dynamic range of less than 8 bits so that at least two exposures would be needed to resolve the energy spread outside the first diffraction lobe. In its place, a Photometeics camera with 14 bits or resolution was used and it is this data which is presented here.

Examples of the data from the 14 bit camera are shown in Fig. 8. In Fig. 8, the difference between a photograph of the yellow HeNe (594nm) reference beam and the laser beam at 16 W on a log scale shows the quality of this data. In Fig. 9, a readout of similar data shows the wavefront reference and 17 W amplified data in a three dimensional format and in Fig. 10 the curves of encircled energy versus beam radius is presented.

Based upon this data, the history of the laser beam quality during the 8 hour run is shown in Fig. 11. The Strehl stayed above 0.6 for most of the run corresponding to a beam quality of ≥ 1.4 times diffraction limited.

Although the two exposure Eltec version of this PIB data was not taken during the run, it was repeated afterwards and the results shown in Fig. 12. Short and long exposures are easily taken with this electronic camera using the variable shutter setting in the camera. The short exposure captures the central portion of the beam with 7-8 bit accuracy while the long exposure images captures 2-3 more bits of dynamic range for the wider angle light. In the longer image, the central lobe is saturated and is masked using the IDL script. However, any beam wander between exposures presents a registration problem and limits the accuracy of this technique. Also, this process is more time consuming and the 14 bit camera technique is recommended.

7. Return flux calculation

Unfortunately there was some ambiguity in the specification on the return flux as set forth in the original contract so that it is not clear whether to use the entire beam, the part of the beam encircling 80% or just the central lobe. Table 1 shows the results of the calculation assuming the 26 kHz repetition rate of the laser, the saturation model for the sodium layer and a one way atmospheric transmission of 70%. The power levels achieved in the burn in test were used but it should be noted that although these power levels were with both three and four YAGS, the fiber lengths were 110 m not the $\approx$ 70 m actually expected. Case B (normal seeing) conditions were used and it was assumed that the beam was circularly polarized which adds another 10-20 % for the 100 ns pulse widths used in the calculation. It is clear that assuming a power level of 20 W, the return flux from both the entire beam and the q_{encl} meet the 0.3 ph/ms/cm^2 criterion.

8. References

1. H. W. Friedman, et. al. "Design of a laser guide star system for the Keck II telescope", Proc. of the ESO Workshop on Laser Technology for Laser Guide Star Adaptive Optics Astronomy, Ed. N. Hubin, Garching, Germany, 23-26 June1997

Acknowledgment

This work was sponsored by the California Association for Research in Astronomy (CARA) through a contract with LLNL. This work was preformed under the auspices of the U.S. DOE by LLNL under contract No. W-7405-Eng-48.

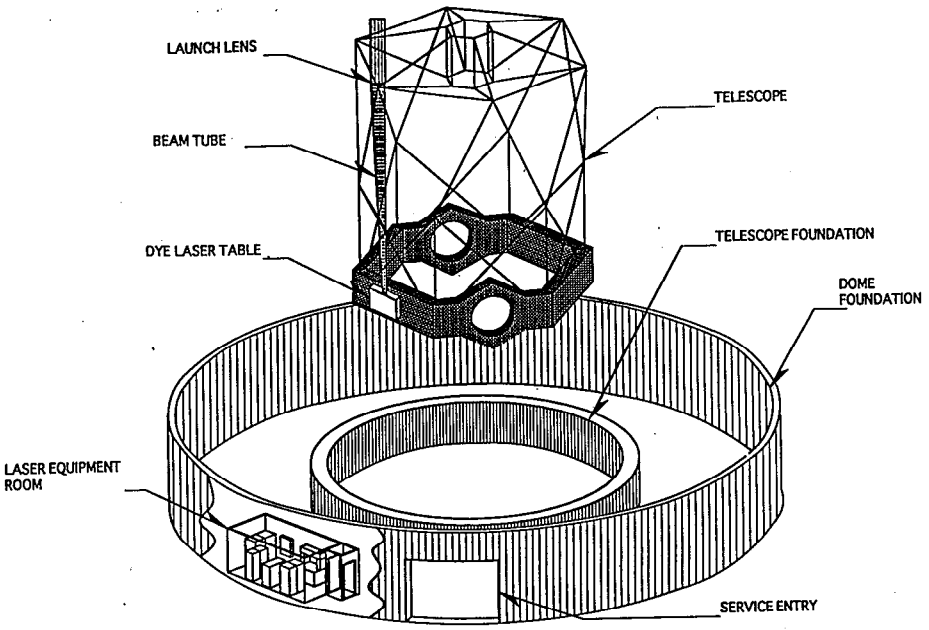

Figure 1. View of the laser system on the Keck II telescope.

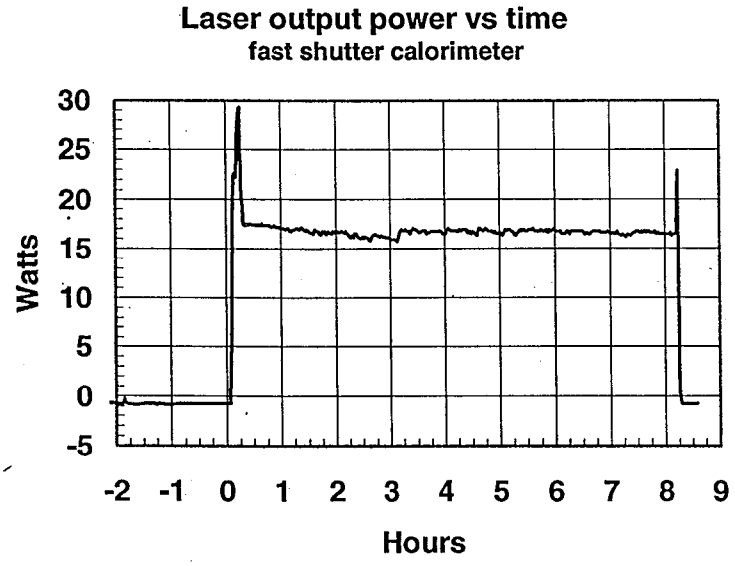

Figure 2. Power reading measured from the fast shutter power meter.

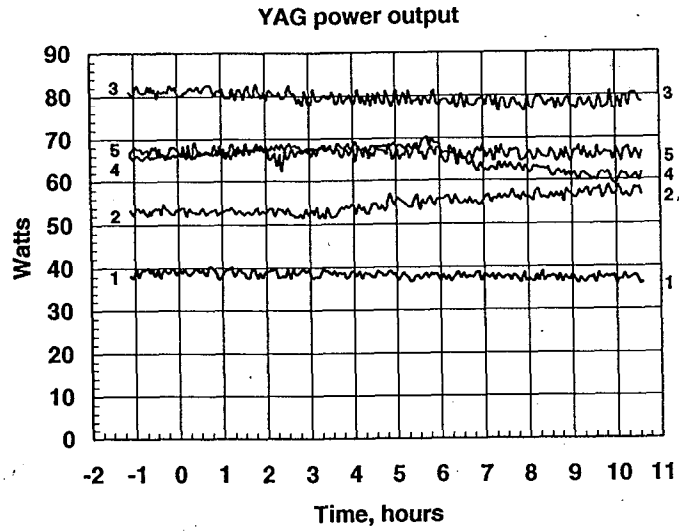

Figure 3. YAG output power as measured in the green before the fiber.

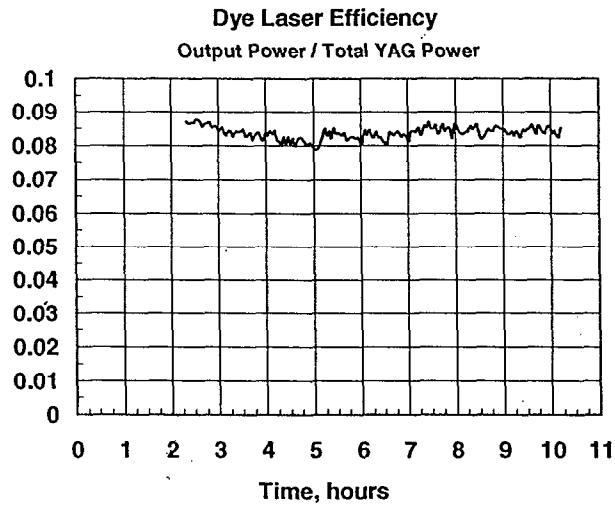

Figure 4. Dye conversion efficiency including the fiber loss.

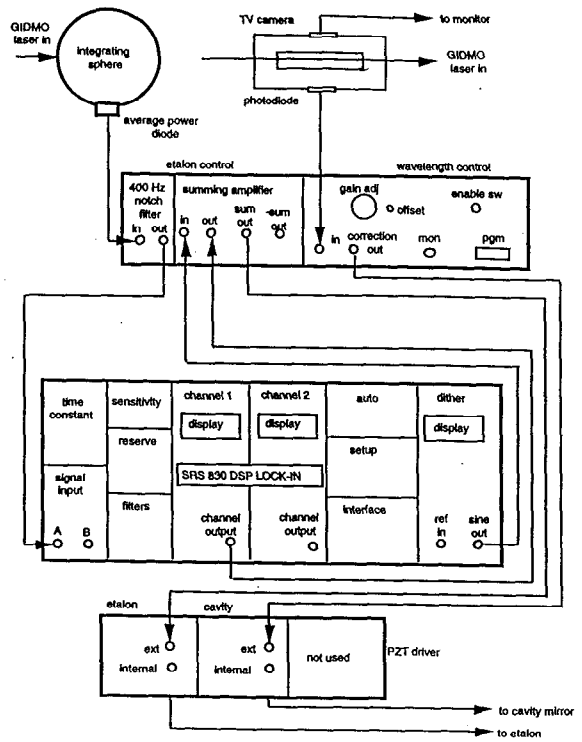

Figure 5. Cabling configuration for the etalon and wavelength lock loops.

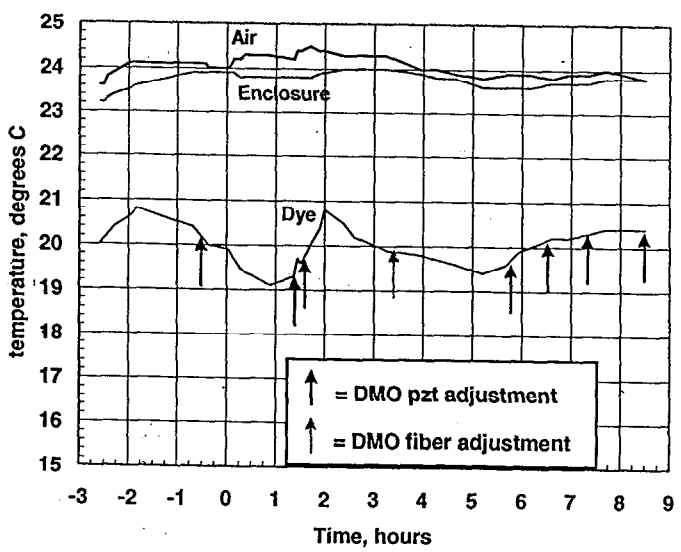

Figure 6. Adjustment to the etalon and wavelength lock loop during the run

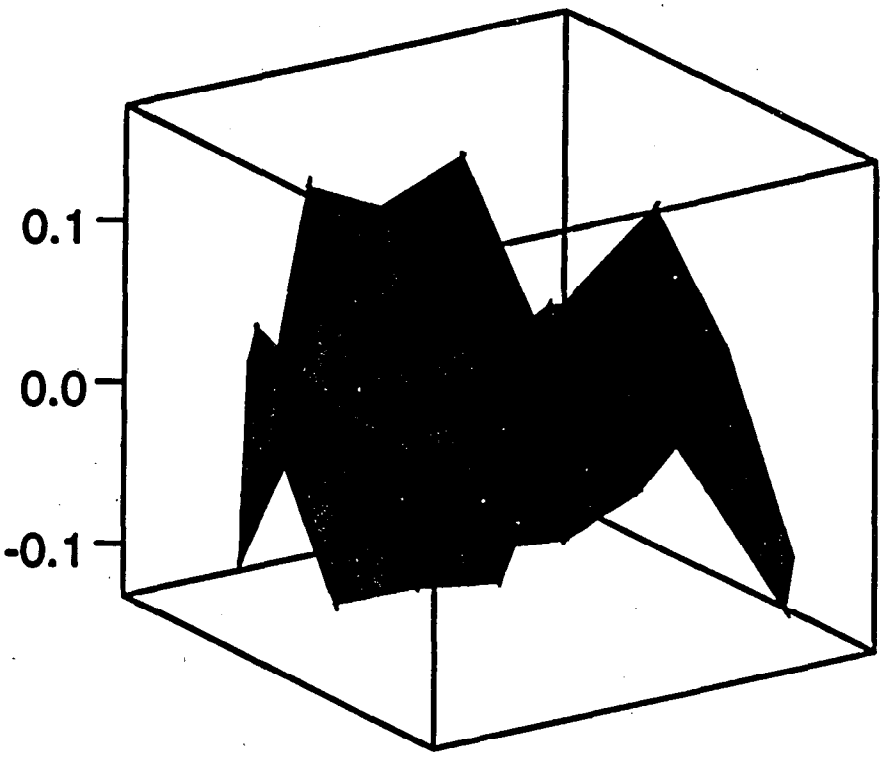

P-V = 0.30 waves
RMS = 0.07 waves
Strehl = 0.832

SagX = -0.01 waves
SagY = 0.15 waves
Angle = -12.70 deg

Shading clipped

16.4 W, Y234, last set

Figure 7. Wavefront map of the entire beam train.

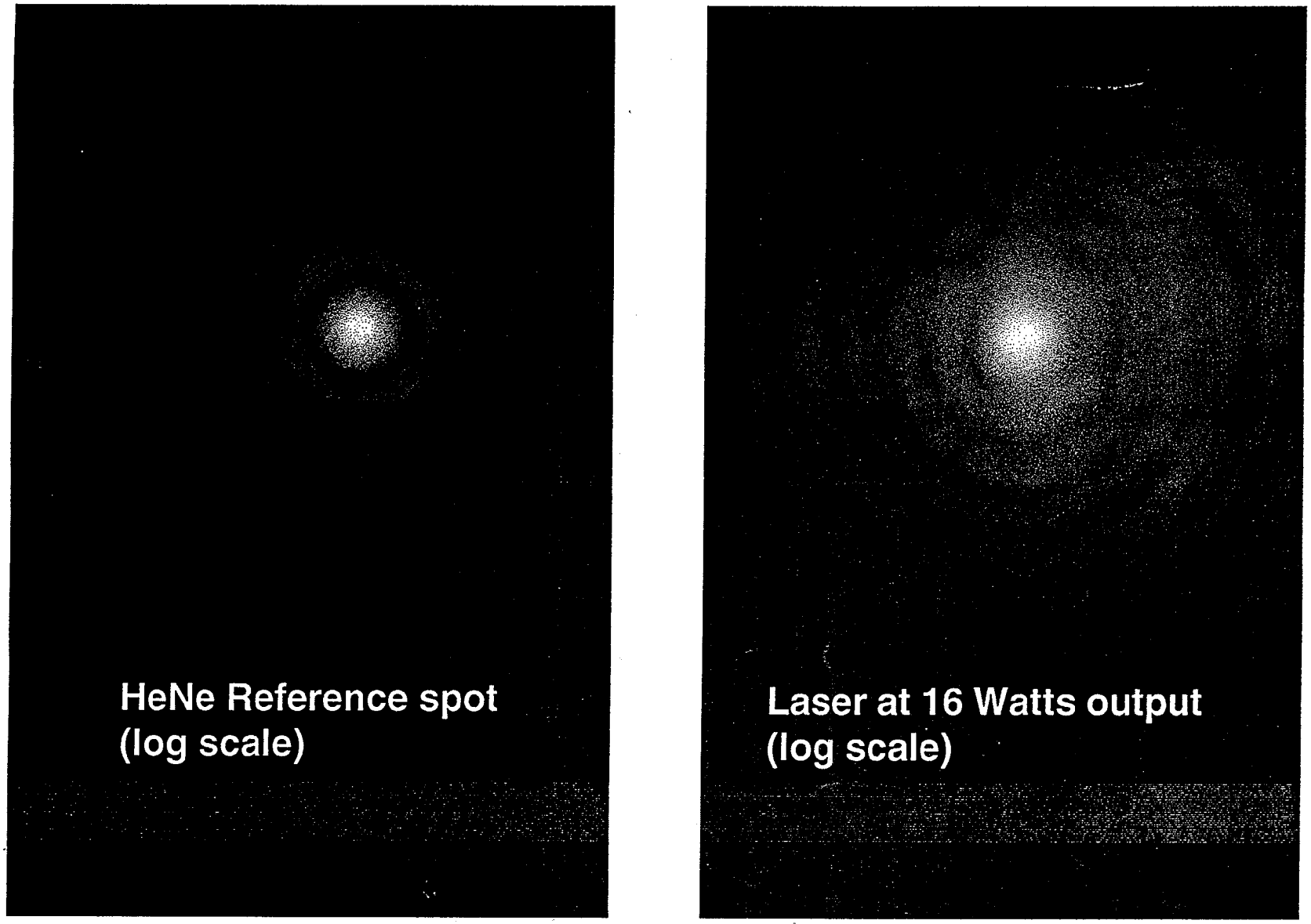

Fig. 8. Log scale photographs of the reference beam and the amplified laser beam.

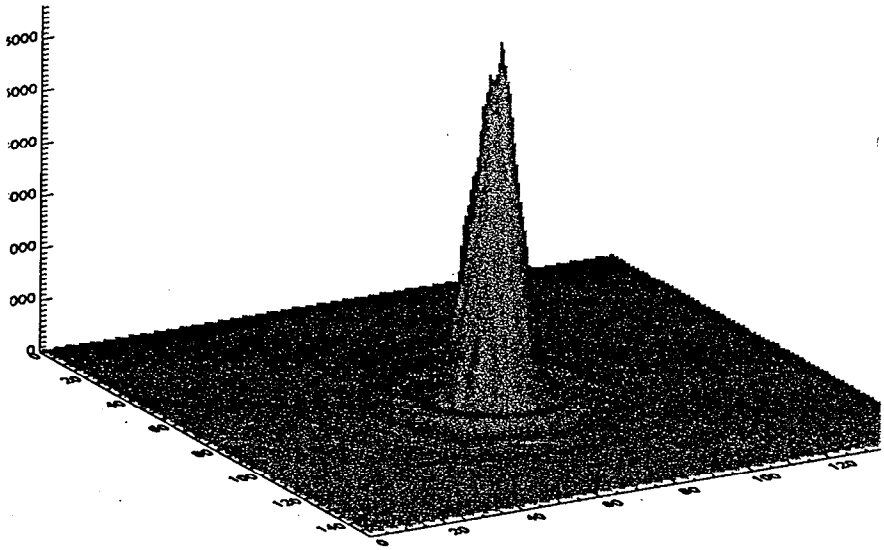

(a) He Ne reference beam

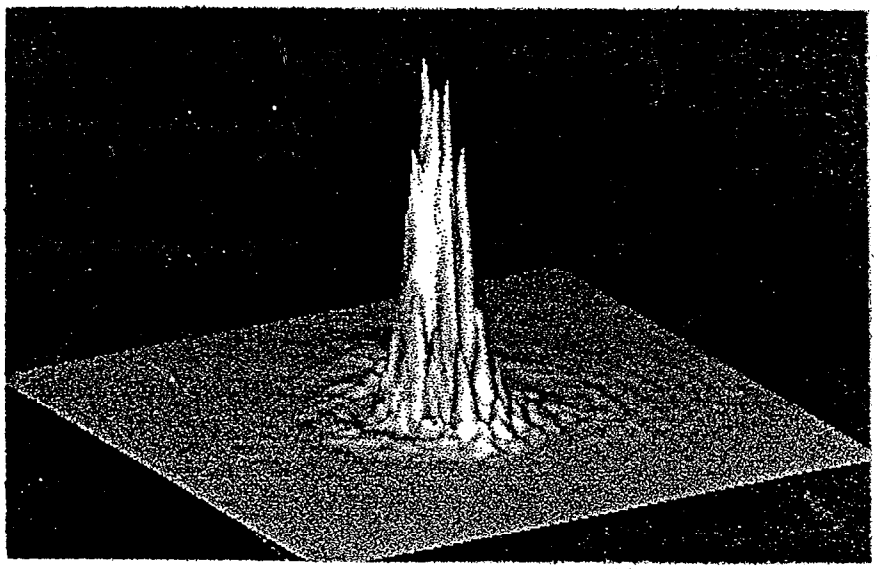

(b) 17 W dye laser beam

Fig. 9. Three dimensional readouts of the data similar to that presented in Fig. 8.

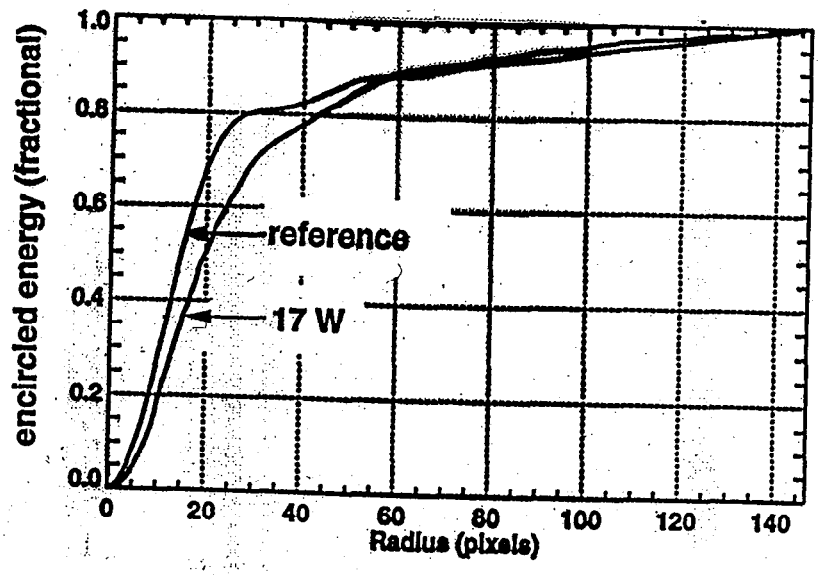

Fig. 10. Encircled energy as a function of beam radius showing a beam quality of $\leq$ 1.4 times diffraction limited.

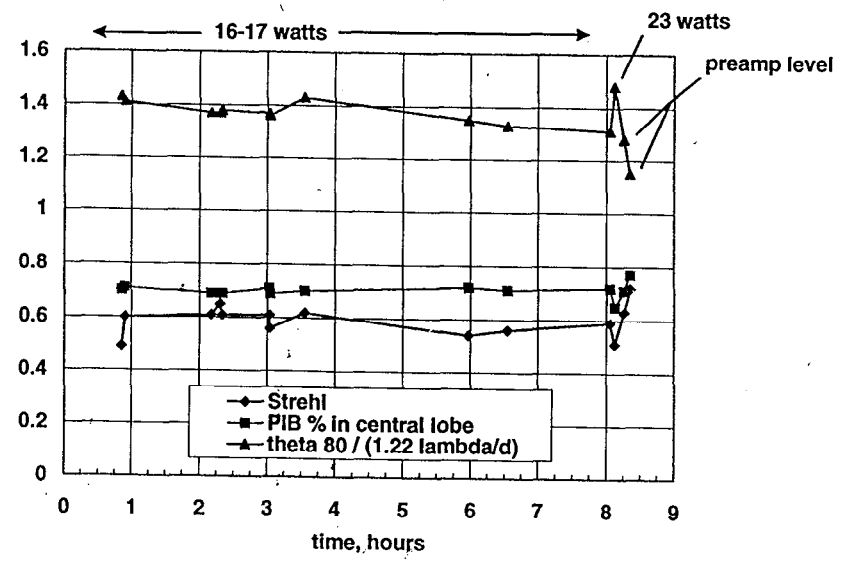

Fig. 11. Beam quality during the 8 hour run.

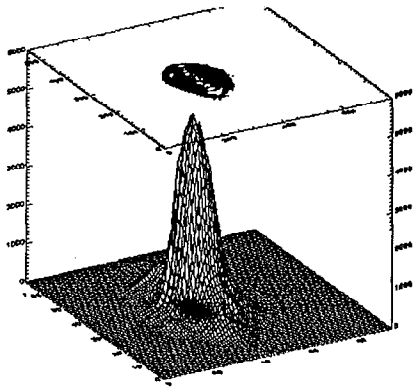

Short exposure image captures the high 7-8 bits

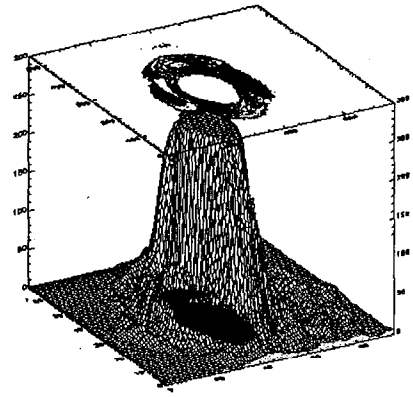

Longer exposure image captures 2-3 more bits of dynamic range, but saturates the central lobe

- **Need to take 2 exposures and combine images, masking the saturated portions of the long exposure image (IDL routine provided)**
- **Any beam wander between exposures presents a registration problem**

Fig. 12. PIB data technique using the 8 bit Eltec camera.

- **Pulse rate = 25 kHz, pulse width = 100 ns**
- **Saturation model for sodium response**
- **70% one way atmospheric transmission assumed**
- **Case B ("normal") seeing conditions assumed**
- **Linear polarization cross-section for Na atom assumed**

laser power	xdl	θ_{encl}	return (ph/ms/cm^2)
	from entire beam		
16 W			0.30
17 W			0.31
23 W			0.37
	from θ_{80}		
16 W	1.4	0.43"	0.26
17 W	1.4	0.43"	0.27
23 W	1.5	0.46"	0.33
	from central lobe		
16 W	1.0	0.31"	0.22
17 W	1.0	0.31"	0.24
23 W	1.0	0.31"	0.26

Table 1. Return flux calculation based upon the results of the 8 hour run.